

Unsteady behaviour of separated and reattaching flows for a backward-facing step configuration at high Reynolds numbers

C. CHOVEL^a, M. LIPPERT^a, L. KEIRSBULCK^a, J-M. FOUCAUT^b.

a. LAMIH UMR8201, Department of Mechanical Engineering, 59313 Valenciennes, France.

camila.chovet@etu.univ-valenciennes.fr

b. LML UMR8107, 59650 Villeneuve d'Ascq, France.

Résumé :

Dans ce travail, nous nous intéressons à la sensibilité des écoulements décollés et rattachés sur une marche descendante à certain paramètres. Des mesures de pression pariétale et de champ de vitesse instationnaires sont effectuées. La longueur de recirculation et le point de décollement secondaire, ainsi que les statistiques de vitesse et de pression ont été analysés et comparés à certaines études antérieures. Les principales caractéristiques de l'écoulement ont été étudiées pour une gamme de nombre de Reynolds allant de 31500 à 182600. L'analyse des spectres de pression instationnaires indiquent que dans la région proche du point de décollement, même pour un nombre de Reynolds élevé, le mouvement de battement basse fréquence est dominant. La compréhension des mécanismes instationnaires ainsi que de leur sensibilités sont un point important en vu du développement de techniques de contrôle actif et / ou passif. Des travaux sont actuellement en cours et ont pour but de définir des stratégies de contrôle actif basées sur la manipulation de ses instabilités.

Abstract :

A contribution to the study of unsteady behavior of separated and reattaching flows over a backward-facing is reported. Unsteady wall pressure and velocity field measurements were done in order to clarify the main Reynolds number dependencies with regards to downstream external parameters. The recirculation length and the secondary separation point, as well as the statistics of the velocity fields and the surface pressure, are analyzed and compared to previous studies. Main flow characteristics were investigated for seven Reynolds numbers ranged from 31500 to 182600. Unsteady pressure spectra analysis indicated that in the region close to the separation point, even for high Reynolds number, the low frequency flapping motion is relatively dominant over the high frequency mode of the large scale vortical structure. The ability to understand the flow field unsteadiness can lead to the development of active and/or passive flow control techniques. Current works are being done searching for active control laws strategies to control these instabilities.

Mots clefs : backward-facing step, turbulent flow, expanding ratio and flapping motion.

1 Introduction

Separating and reattaching flows can be found in many practical engineering applications. More recently, control strategies have been actively studied to improve performance in these flows. The ability to understand the flow field can lead to the development of active and/or passive flow control techniques. These unstable flows can be classified in two distinct classes [1] : hydrodynamic oscillators (absolutely unstable) and noise amplifiers (absolutely stable but convectively unstable). In hydrodynamic oscillators, instabilities grow *in situ* and survive for all time. For amplifier flows, the basic flow carries growing perturbations away in the downstream direction, and the system eventually returns to its unperturbed state. These flows are very sensitive to external perturbations and their characteristics determine the type of waves amplifying the flow [2].

One of the most commonly amplifier configurations is the backward-facing step. The flow over a backward-facing step (BFS) represents a geometrically simple canonical flow situation exhibiting both separation and reattachment. Many studies were conducted at low Reynolds numbers $Re_h = 10^4$ (Chung and Sung [3], Nadge and Govardhan [4], Hudy et al. [5]), but only few of them were carried out at moderate- and high Reynolds numbers (Heenan and Morrison [6]). What remains to determine is the Reynolds number dependency to external parameters e.g., expanding ratio Er and boundary layer δ/h , and the nature of turbulent flows, specifically at $Re_h > 10^4$. Most practical flows are turbulent, and are furthermore complicated by strong large-scale vortices or recirculation.

The present study aims to clarify the main separate dependencies of the flow over a wide range of Reynolds numbers regarding downstream external parameters (e.g., expanding ratio Er and boundary layer δ/h). The recirculation length and the secondary separation point, as well as the statistics of the velocity fields and the surface pressure, were analyzed and compared to previous studies. This comparison was done to understand the influence of incoming boundary layer thickness and wall-bounded effect associated with high expanding ratio.

2 Experimental apparatus

Experiments took place in a closed-loop wind tunnel with a $2m \times 2m \times 10m$ test section. The model is mounted in the middle of the test section and exactly fits the spanwise. The step height of the backward-facing step is 83mm and corresponds to an expansion ratio of 1.04, i.e. negligible inference of the upper wall. An effectively nominally two-dimensional flow is provided by the large span of 2000mm yielding an aspect ratio of 24 [7]. Measurements were performed at various free stream velocities in the range of $U_\infty = 5.7 - 33.0m/s$ corresponding to a Reynolds number range of $Re_h = 31500 - 182600$ based on the step height and the free stream velocity. The origin of the co-ordinate system is located at the edge of the step. The x-axis represents the stream wise flow direction, the y-axis the normal direction to the flow and the z-axis the spanwise or cross-stream flow. In order to represent the exposed parts described above, a sketch of the experimental is shown in Fig. 1.

Static pressure taps were distributed downstream of the back-facing step in the freestream direction. The 25 pressure tabs were mounted starting at 25mm from the step with an interval between each other of 50 mm ($x/h = 0.6$), as shown in Fig. 1. In addition, a second set of 25 sub-miniature piezo-resistive Kulite XCQ-062 sensors (Flush-mounted Kulite transducers) were placed in parallel and at the same x location as the static ones. These sensors have a nominal measurement range of 35 kPa. The 25 unsteady and static pressure sensor rows extended up to $14.75H$ in the streamwise direction.

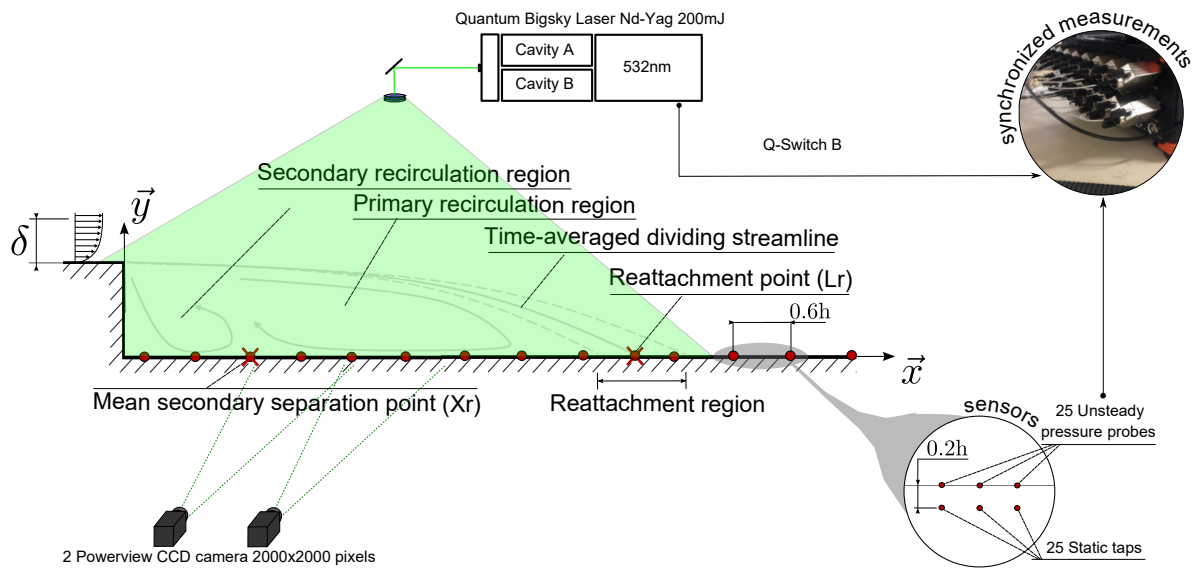
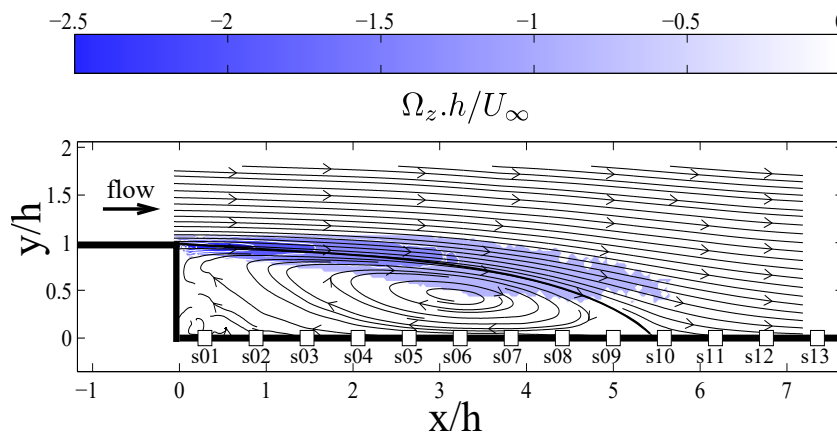


FIGURE 1 – Experimental setup of a backward-facing step flow.

FIGURE 2 – Non-dimensional, mean vorticity $\Omega_z \cdot h / U_\infty$ and associate streamlines for $Re_h = 64200$. Dark line denotes the streamline originated at the step edge, i.e., $x=0, y=h$

Velocity measurements were performed downstream of the step with a standard two-component TSI particle image velocimetry (PIV). The PIV field of view is about $7.3h \times 1.8h$ on the x - y plane and passes through the backward facing step center. The system consists of a double-pulse laser system and two cameras (2000×2000 pixels charge-coupled-device Powerview with a 50 mm optical lens). The frequency-doubled laser (Qswitched Nd :YAG operating at 532 nm; dual-head BigSky) emits laser pulses with a maximum energy of 200 mJ. The camera resolution is 19.2 pixels/mm. The dynamic range is approximately 30 pixels and the velocity vectors are processed with an interrogation window of 16×16 pixels with 50% overlap. For every flow/actuation configurations, 2000 double-frame pictures were recorded to ensure the velocity fields statistics convergence. The PIV time-uncorrelated snapshots were registered with a repetition rate of 7 Hz. The velocity measurements were sampled at 10kHz and latter filtered at 3kHz.

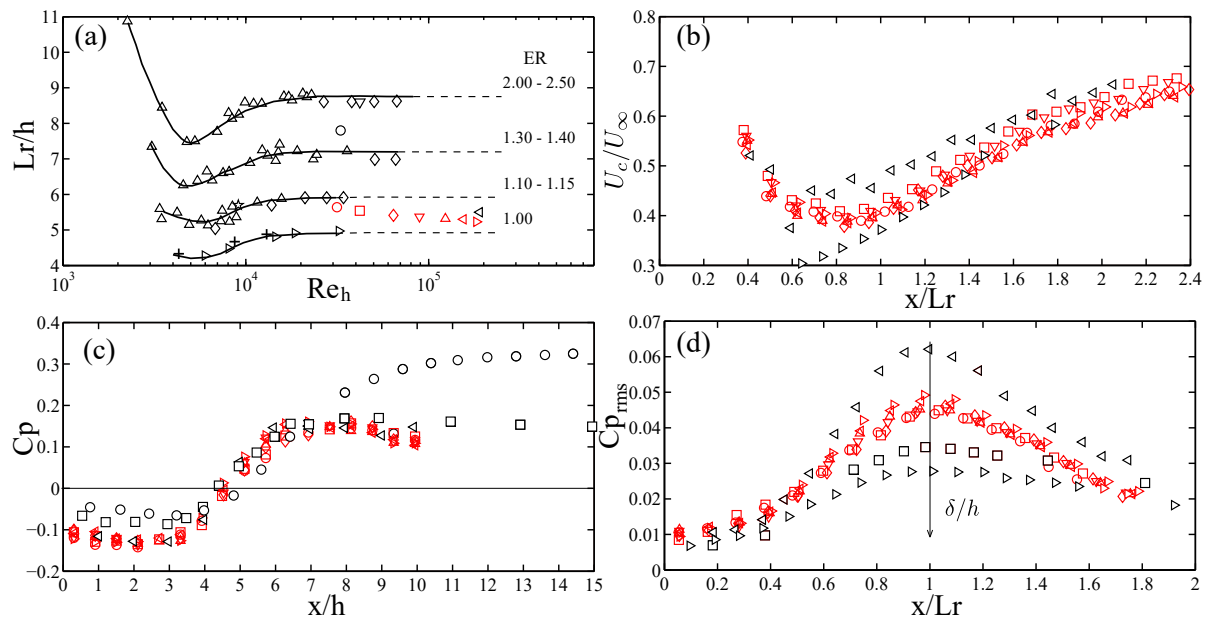


FIGURE 3 – (a) Recirculation lengths against Re_h for various ER . Authors from Table 1 are also reported; (b) Convection velocities from wall-pressure measurements for all the Reynolds numbers studied, results are compared with the data of Heenan and Morrison [6] and Hudy *et al.* [5]; (c) Mean pressure coefficients from present and previous studies reported in Table 1; (d) Rms pressure coefficients from present and previous studies reported in Table 1 for ER between 1.10 and 1.15

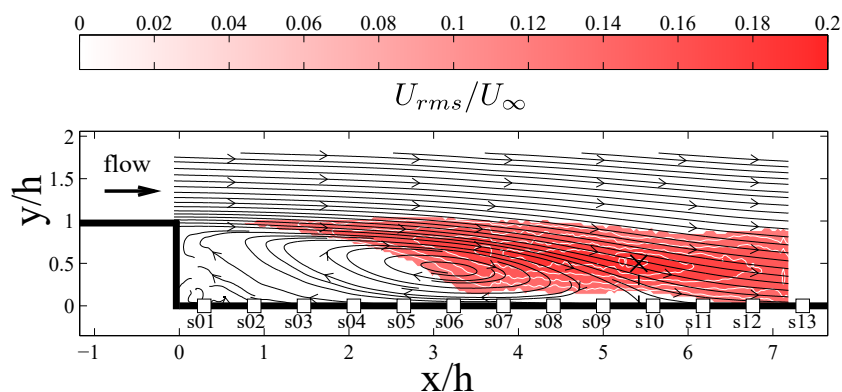


FIGURE 4 – Contour map of the streamwise rms-velocity (U_{rms}/U_∞) for $Re_h = 64200$ with associated streamlines. Black cross symbol denotes the maximum rms-velocity location

TABLE 1 – Mean-flow parameters for various authors

Authors	Re_h	δ/h	ER	L_r/h	Symbols
Chung and Sung, 1996 [3]	33000	0.38	1.50	7.80	○
Driver and Seegmiller, 1985 [8]	37420	1.50	1.12	6.1±1.0	□
Westphal and Johnston, 1984 [9]	42000	0.40	1.67	8.60	▽
Durst and Tropea, 1981 [10]	1800-30000	-	1.06-2.05	5.0-11.0	△
Nadge and Govardhan, [4]	5000-64000	0.18-0.76	1.10-2.50	5.0-8.8	◇
Li and Nagib, 2005 [11]	4300-13000	-	1.00	4.3-4.8	+
Heenan and Morrison, 1995 [6]	190000	0.21	1.10	5.50	◁
Hudy et al., 2007 [5]	5980-32327	-	1.00	4.3-4.9	▷
Li et al., 2015 [12]	9100	0.12	1.08	5.7	☆
Chovet et al. (present study)	31500	0.68	1.04	5.62	○
	42000	0.63	1.04	5.54	□
	64200	0.57	1.04	5.41	◇
	89100	0.53	1.04	5.37	▽
	123400	0.50	1.04	5.32	△
	154900	0.48	1.04	5.30	◁
	182600	0.47	1.04	5.23	▷

3 Flow statistics and dependencies

Flow characteristics were investigated for seven Reynolds numbers (Tab. 1). As an example, the non-dimensional mean vorticity field in the x-y plane, $\Omega_z \cdot h / U_\infty$, with associated streamlines for $Re_h = 64200$, is plotted in Fig. 2. The contour map of the mean spanwise vorticity underlines the boundary layer separation at the edge of the step. The formed shear layer is detached from the step, increasing in width throughout the streamwise direction, to finally reattach upstream the step. The shear layer is distributed predominantly around the mean separation streamline and is globally represented in Fig. 2 as the negative vorticity region. The mean separation streamline, originated at the step edge, i.e., $x=0$, $y=h$, and denoted as a dark line, impacts the surface at the mean reattachment point. Beneath the shear layer, a primary re-circulating region and a secondary re-circulation bubble (closer to the step corner) are also observed.

The experimental investigations described herein address the backward facing-step flow dependencies regarding the Reynolds number and the expanding ratio (ER). Fig. 3(a) shows a compilation of some previous works reported in Table 1. Most of these works refer to moderate Reynolds numbers and only a few of them cover high Reynolds numbers ($Re_h \geq 10^5$). Present results, reported in Fig. 3(a) by red symbols, showed a decrease of the mean reattachment length when the Reynolds number increases, in other word, for high Reynolds numbers there is no constant trend, as stated by Nadge and Govardhan [4], but a decrease of the recirculation length due to another parameter, as also seen by Heenan and Morrison [6]. For higher Reynolds numbers, the reattachment length dependency with the Reynolds number disappears but the expansion ratio becomes relevant in the determination of this length.

The convection velocities deduced from wall-pressure space-time correlations are seen in Fig. 3(b). Results show a decrease of the convection velocities from $0.6 \approx U_\infty$, near the step edge, to $0.4U_\infty$, at $x = 0.8L_r$. After this point, values increase almost linearly. For the present study, the convection velocities appear to reach a minimum value near the position where the mean pressure coefficient is equal to zero $x = 5h$. A good qualitative agreement with Heenan and Morrison [6] and Hudy et al. [5]

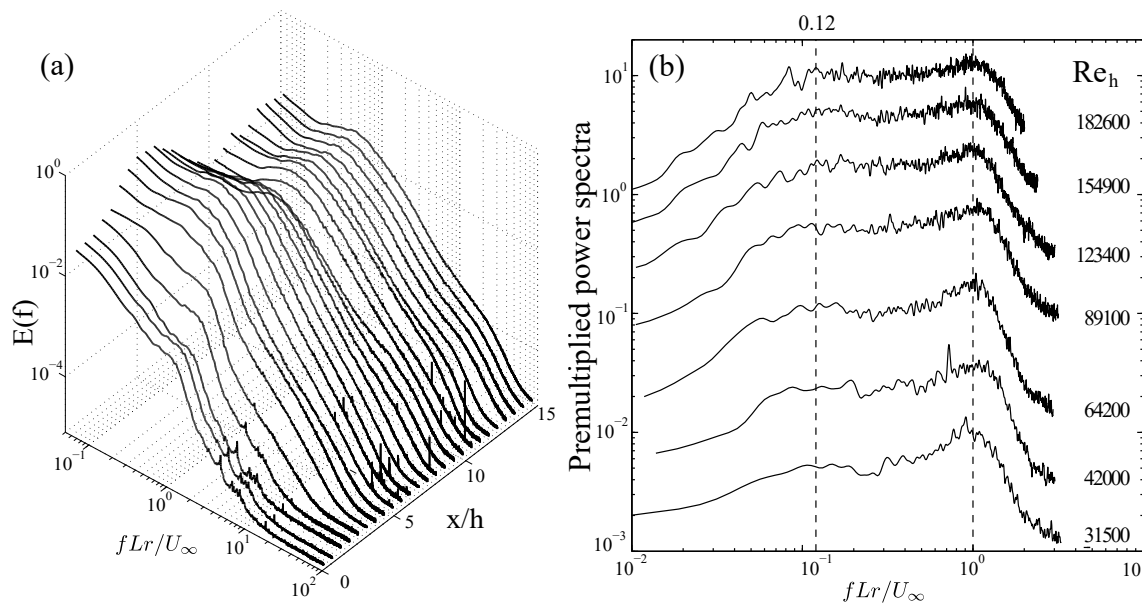


FIGURE 5 – (a) Power spectra of wall-pressure fluctuations for different x/h locations at $Re_h = 64200$; (b) Non-dimensional premultiplied power spectra of fluctuating wall pressure measured at $x/h = 1.5$ for various Reynolds numbers.

is observed, regardless of the Reynolds numbers. Nevertheless, the data from Heenan and Morrison and Hudy seem to reach minimum values lower than those obtained in our case.

In the same way, the mean-pressure coefficient is plotted in Fig. 3(c). This coefficient is defined as $C_p = (P - P_{ref}) / (1/2\rho U_\infty^2)$, with P the pressure measured along the surface of the model and P_{ref} a reference pressure measured with a static-pressure tap located upstream the step edge. Immediately downstream of the step a positive peak is clearly seen at $7h$. The present results are in agreement with those obtained by Heenan and Morrison [6].

Present and previous rms pressure coefficients, defined as $C_{p_{rms}} = p_{rms} / (1/2\rho U_\infty^2)$, are shown in Fig. 3(d) as a function of x/L_r . The global behavior of the rms pressure distribution, obtained in the present work, is consistent with the findings of Castro and Haque [13] and Hudy *et al.* [5]. A peak in the rms pressure distribution is clearly observed for both past and present studies. For the same ER ($\approx 1 - 1.1$), the locations of the peaks are similar and situated near the reattachment point ($X/L_r = 1$). In addition, the location of the maximum rms pressure coefficient is strongly linked to the maximum streamwise rms-velocity, as denoted in Fig. 4 with a cross symbol. This near-wall interdependence, reattaching shear-layer structure and wall rms-pressure in the reattachment region, is due to shear layer structures convecting downstream and producing an increasingly strong wall-pressure signature. This signature reaches a maximum level near the location where the flow “impinges” onto the wall, as described by Farabee and Casarella [14].

Fig. 5(a) shows a log-log plot of the pressure fluctuations spectra at several x/h locations downstream the step at $Re_h = 64200$. Four different regions can be identified and showed the global behavior of the flow downstream the backward-facing step. The first region, from the step edge to $x/h \approx 1.5$ ($x/L_r < 0.3$), shows a low pressure fluctuations where the spectra are dominated by both low- and high-frequency fluctuations. A second region, where a transition occurs from the previous frequency peaks, at $x/h \approx 1.5$ ($x/L_r \approx 0.3$), to a merged frequency value at $x/h \approx 4.5$ ($x/L_r < 0.8$). The third one, corresponding to the recirculation region from $x/h \approx 4.5$ to 6.5 , where the pressure fluctuations are strong and the high

energy levels are clearly visible ; this behavior is consistent with the pressure coefficient results in Fig. 3(d). The last region represents the reattached zone where the behavior approaches a typical turbulent boundary layer spectrum. This global mechanism is also reported for the same configuration but for low Reynolds numbers by Spazzini *et al.* [15].

Finally, in order to analyze the behavior of the low frequencies in the flow field and their Reynolds number dependency, premultiplied pressure fluctuation power spectra were evaluated at $x/h = 1.5$ from the step edge, where the flow is clearly dominated by these low frequencies. Present results are shown in Fig. 5(b) for all Reynolds number. Two frequency peaks can be observed. The first one $f.L_r/U_\infty = 0.12$ corresponds to a classical well-defined flapping frequency, and a higher one at around $f.L_r/U_\infty = 1$ related to the shedding phenomena. Flow field dynamics will be further studies, using Proper Orthogonal Decomposition (POD) to thoroughly analyse the dynamical aspect of the flow fields for a wide range of Reynold numbers.

4 Conclusions

Unsteady characteristics of the wall-pressure fluctuations and velocity field over a backward-facing step have been described. Previous experimental data in a similar configuration were compared to present results to clarify the flow dependency on external parameters, e.g., Reynold number and expanding ratio. Only a few experiments at high Reynolds numbers ($Re_h > 10^5$) have been done. In the former conditions, the recirculation length dependency on the Reynolds number disappears as stated in previous experiments. However, results show that there is no constant trend after $Re_h > 10^5$ but a decrease in the recirculation length, meaning that this reattachment point depends on other parameters. It is possible to highlight that, for high Reynolds numbers, the expanding ratio dependency becomes relevant in the determination of the recirculation length. Finally, the premultiplied power spectra of the pressure fluctuations exhibit two main peaks : one corresponding to the flapping frequency and a second peak related to the shedding phenomena. Future analysis will be done to deeply understand the statistically dominant structures of the flow. The knowledge of these instabilities presented at high Reynolds numbers opens the door to create passive and active laws to control the flow.

Acknowledgment

This work was carried out within the framework of the CNRS Research Federation on Ground Transports and Mobility, in articulation with the ELSAT2020 project supported by the European Community, the French Ministry of Higher Education and Research, the Hauts de France Regional Council. The authors gratefully acknowledge the support of these institutions.

Références

- [1] P. Huerre, M. Rossi , Hydrodynamic instabilities in open flow, In Hydrodynamic and Nonlinear Instabilities Cambridge university Press, (1998) 81–294.
- [2] B. Pier, P. Huerre, Nonlinear synchronization in open flows, Journal of Fluids and Structures, Elsevier, 15 (2001) 471–480.
- [3] K.B. Chung, H.J. Sung, Control of turbulent separated flow over a backward-facing step by local forcing, Exp in Fluids, 21 (1996) 417–426.

- [4] P.M. Nadge, R.N. Govardhan, High Reynolds number flow over a backward-facing step : structure of the mean separation bubble, *Exp. Fluids*, 55 (2014) 1657.
- [5] L.M. Hudy, A. Naguib, W.M. Humphreys, Stochastic estimation of a separated-flow field using wall-pressure-array measurements, *Phys Fluids*, 19 (2007) 024103 .
- [6] A.F.Heenan, J.F. Morrison, Passive control of pressure fluctuations generated by separated flow, *AIAA Journal*, 36 (1998) 1014–1022.
- [7] V. De Brederode, P. Bradshaw, Influence of the side walls on the turbulent centerplane boundary-layer in a squareduct, *Trans. ASME I : J. Fluids Eng.*, 100 (1978) 91–96.
- [8] D.M. Driver, H.L. Seegmiller, Features of a reattaching shear layer in divergent channel flow, *AIAA Journal*, 23(2) (1985) 163–171.
- [9] R.V. Westphal, J.P. Johnston, Effect of initial conditions on turbulent reattament downstream of a backward-facing step, *AIAA Journal*, 22 (1984) 1727–1732.
- [10] F. Durst, C. Tropea, Turbulent backward-facing step flows in two-dimensional ducts and channels, *Proceedings of turbulentshear flow 3 symposium Davis*, (1981).
- [11] Y. Li, A.M. Naguib, High-Frequency Oscillating-Hot-Wire Sensor for Near-Wall Diagnostics in Separated Flows, *AIAA Journal*, 25(3) (2005) 520–529.
- [12] Z.Li, H. Bai, N. Gao, Response of turbulent fluctuations to the periodic perturbations in a flow over a backward-facing step, *Th. Applied Mech. Letters*, 5 (2015) 191–195.
- [13] P. Castro, A. Haque, The structure of a turbulent shear layer bounding a separation region, *J. Fluid Mech.*, 179 (1987) 439.
- [14] M. Farabee, M.J. Casarella, Measurements of fluctuating wall pressure for separated/reattached boundary layer flows, *ASME J. Vib., Acoust., Stress, Reliab. Des.*, 108(1986) 301.
- [15] P.G. Spazzini, G. Iuso, M. Onorato, N. Zurlo, G.M.Di Cicca, Unsteady behavior of back-facing step flow, *Exp. Fluids*, 30 (2001) 551–561.